JOURNAL OF AGRICULTURAL AND FOOD CHEMISTRY

Article

pubs.acs.org/JAFC

# Molecularly Imprinted Photonic Hydrogels as Colorimetric Sensors for Rapid and Label-free Detection of Vanillin

Hailong Peng,[†,‡] Shenqi Wang,[†,∥] Zhong Zhang,[†,∥] Hua Xiong,[*,†] Jinhua Li,[§] Lingxin Chen,[§] and Yanbin Li[⊗,⊥]

[†]State Key Laboratory of Food Science and Technology, Nanchang University, Nanchang 330047, China

[‡]Department of Chemical and Pharmaceutical Engineering, Nanchang University, Nanchang 330031, China

[§]Key Laboratory of Coastal Zone Environmental Processes, Yantai Institute of Coastal Zone Research, Chinese Academy of Sciences, Yantai 264003, China

[⊗]College of Biosystems Engineering and Food Science, Zhejiang University, Hangzhou 310058, China

[⊥]Department of Biological and Agricultural Engineering, University of Arkansas, Fayetteville, Arkansas 72701, United States

**ABSTRACT:** A novel colorimetric sensor for the rapid and label-free detection of vanillin, based on the combination of photonic crystal and molecular imprinting technique, was developed. The sensing platform of molecularly imprinted photonic hydrogel (MIPH) was prepared by a noncovalent and self-assembly approach using vanillin as a template molecule. Morphology characterization by scanning electron microscope (SEM) showed that the MIPH possessed a highly ordered three-dimensional (3D) macroporous structure with nanocavities. The vanillin recognition events of the created nonocavities could be directly transferred into readable optical signals through a change in Bragg diffraction of the ordered macropores array of MIPH. The Bragg diffraction peak shifted from 451 to 486 nm when the concentration of the vanillin was increased from $10^{-12}$ to $10^{-3}$ mol $L^{-1}$ within 60 s, whereas there were no obvious peak shifts for methyl and ethyl vanillin, indicating that the MIPH had high selectivity and rapid response for vanillin. The adsorption results showed that the hierarchical porous structure and homogeneous layers were formed in the MIPH with higher adsorption capacity. The application of such a label-free sensor with high selectivity, high sensitivity, high stability, and easy operation might offer a potential method for rapid real-time detection of trace vanillin.

**KEYWORDS:** *vanillin, colorimetric detection, molecular imprinting, photonic hydrogel*

## INTRODUCTION

Vanillin is a unique and highly prized flavor compound widely used in the flavoring of many foods such as ice cream, bakery items, and fruits. Although vanillin can enhance the scent of foods, it is a synthetic perfume and food additive. If large amounts are ingested into the body, vanillin causes headaches, nausea, and vomiting and could also affect liver and kidney functions.[1] Hence, the determination of vanillin contents plays an important role in food fields. Generally, the widely used analytical methods for vanillin are chromatography and spectrometry, such as the AOAC method,[2] gas chromatography–liquid chromatography–mass spectrometry (GC-LC-MS),[3] high-performance liquid chromatography (HPLC),[4] and capillary electrophoresis (CE).[5] However, these methods suffer from some drawbacks: they are time-consuming and expensive and have low sensitivity. Also, most of them often need complicated pretreatment procedures. All of these impose restrictions on their applications for vanillin detection. Therefore, the development of simple, rapid, highly selective, and sensitive analytical methods is urgently required.

Because of their unique properties of structure predictability, recognition specificity, and application universality, molecularly imprinted polymers (MIPs) have received great attention and become a research hotspot.[6] MIPs are highly cross-linked porous-rich polymers with specific recognition sites complementary in shape and size, and the created nanocavities can act as artificial antibodies and exhibit high selectivity toward the imprinted molecules (template).[7] On the other hand, MIPs have other advantages such as physical robustness, thermal stability, low cost, and easy preparation.[8] Consequently, MIPs are being extensively studied and widely applied for solid-phase extraction (SPE),[9] chromatographic separation,[10] and chemo/biosensors.[11−13] Recently, MIPs were also widely applied in food fields for enrichment,[14] separation,[15] and determination of analytes.[16] MIPs as sorbents to separate and enrich analytes could solve the problem of lack of selectivity, but expensive and sophisticated instruments with long experimental times are usually needed.[17] Thus, the development of MIP-based label-free and rapid analytical methods for on-site determination of analytes in foods is highly desirable.

On the basis of the highly three-dimensional (3D) ordered interconnected macroporous structure and interesting optical properties, photonic crystals have drawn considerable attention for the development of various chemical and biological sensors.[18] Photonic crystals exhibit fascinating Bragg diffraction and bright structural colors due to the periodic porous structure.[19,20] Recently, photonic crystals have been applied to create macroporous hydrogels with highly ordered 3D structures combining with MIPs.[21−23] The optical properties of

Received: November 19, 2011
Revised: January 31, 2012
Accepted: February 1, 2012
Published: February 1, 2012

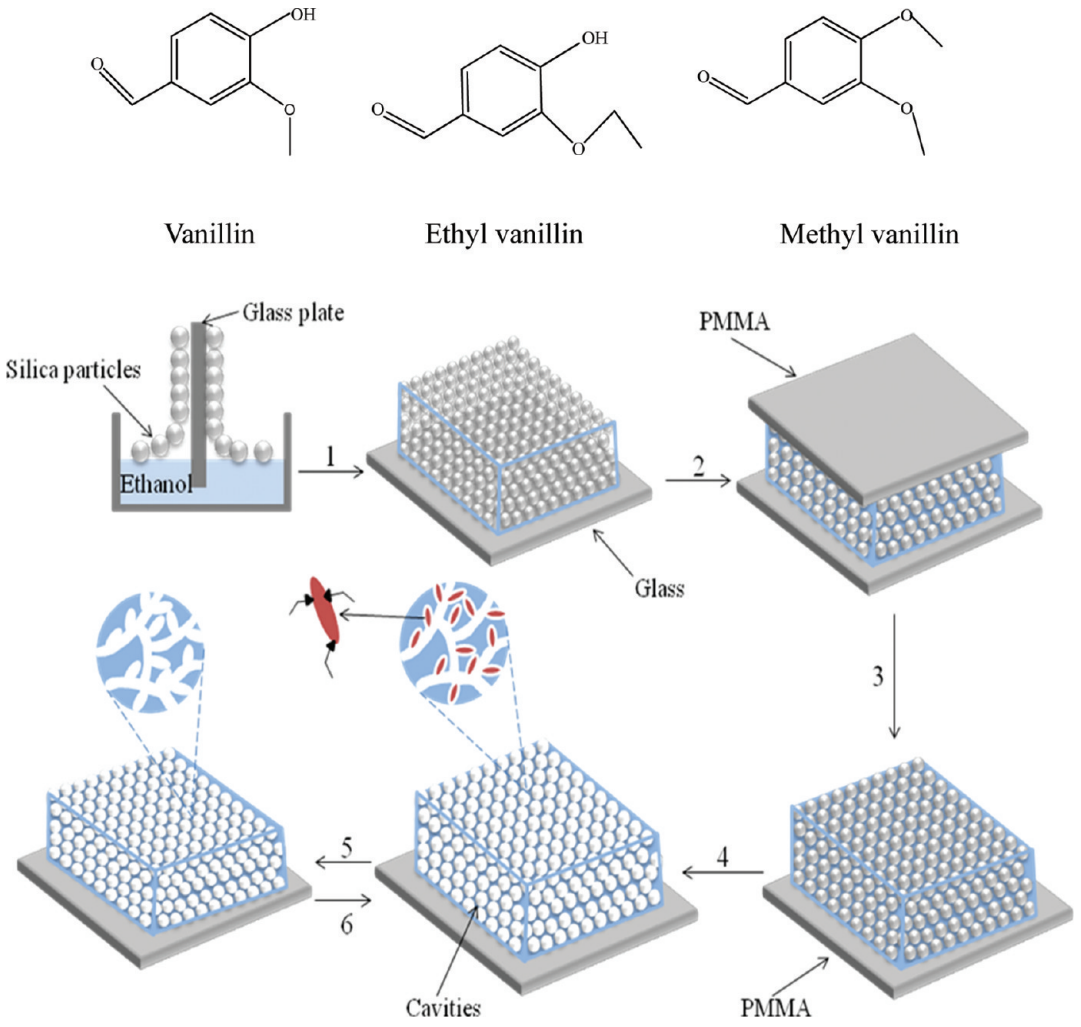


**Figure 1.** (Top) Chemical structures of vanillin and its analogues used. (Bottom) Schematic illustration of the procedure used for preparation of MIPH: 1, preparation of silica colloidal crystals molding on glass substrate; 2, preparation of "sandwich structure" and infiltration with precursor solution; 3, photopolymerization; 4, removal of silica particles using hydrofluoric acid; 5, removal of vanillin using methanol; 6, rebinding of vanillin.

the highly ordered 3D macroporous hydrogel could be changed with swelling or shrinking of the hydrogel volume. It is interesting that the change in optical properties could be transferred into a readable optical signal accompanying a visual color. On the basis of the unique properties of photonic crystals and MIPs, combining molecular imprinting with photonic hydrogels is an emerging and promising technique, and the corresponding sensor platforms have been developed to measure various chemical and environmental stimuli, such as pH,[24] metal ions,[25,26] and humidity.[27] However, to the best of our knowledge, until now, there have been few reports on the application of such sensors for efficient detection of analytes in food fields based on the combination of molecular imprinting and photonic hydrogels.

In this work, vanillin was selected as a template for molecularly imprinted photonic hydrogels (MIPHs). Molecular imprinting and photonic hydrogels were combined in an effort to develop a convenient and efficient photonic-based sensor system for the rapid and label-free colorimetric detection of vanillin. The morphology and optical properties of the MIPH were systematically investigated, as were the sensitivity, selectivity, responsibility, recoverability, and stability. The developed platform may provide a novel approach for the monitoring and detection of trace vanillin in foods without the need for labels and expensive instruments.

## EXPERIMENTAL PROCEDURES

**Reagents and Materials.** Vanillin, methyl vanillin, and ethyl vanillin were purchased from Shanghai Chemical Reagents Co. (Shanghai, China). Their structures are shown in Figure 1. Ethylene glycol dimethylacrylate (EGDMA), methacrylic acid (MAA), and 2,2′-azobis(isobutyronitrile) (AIBN) were all purchased from Sigma-Aldrich (Shanghai, China). Tetraethoxysilane (TEOS) was obtained from Aladdin (Shanghai, China). Other affiliated chemicals were all obtained from Donghu Chemical Reagents Co. (Nanchang, China). All reagents used were of analytical grade. Buffer solution ($NaH_2PO_4$/$Na_2HPO_4$, pH 7.6) was prepared for tests. The deionized water used was produced by a Milli-Q Ultrapure water system with the water outlet operating at 18.2 MΩ (Millipore, Bedford, MA).

**Glassware Treatment.** All of the small glass instruments (glass slides, round flasks, test tubes, etc.) were treated with and immersed in $H_2SO_4/H_2O_2$ (7:3, v/v) solution for 24 h. After that, this glassware was rinsed with deionized water and anhydrous ethanol in the ultrasonic bath, respectively, and then dried for use. Polymethyl methacrylate (PMMA) slides as supports for the formed MIPH film were cleaned with anhydrous ethanol.

**Synthesis of Silica Particles.** The monodisperse silica particles were synthesized according to the Stöber method[28] with necessary modifications as follows. Ethanol (150 mL) was put into a round flask,


dx.doi.org/10.1021/jf204736p | J. Agric. Food Chem. 2012, 60, 1921−1928

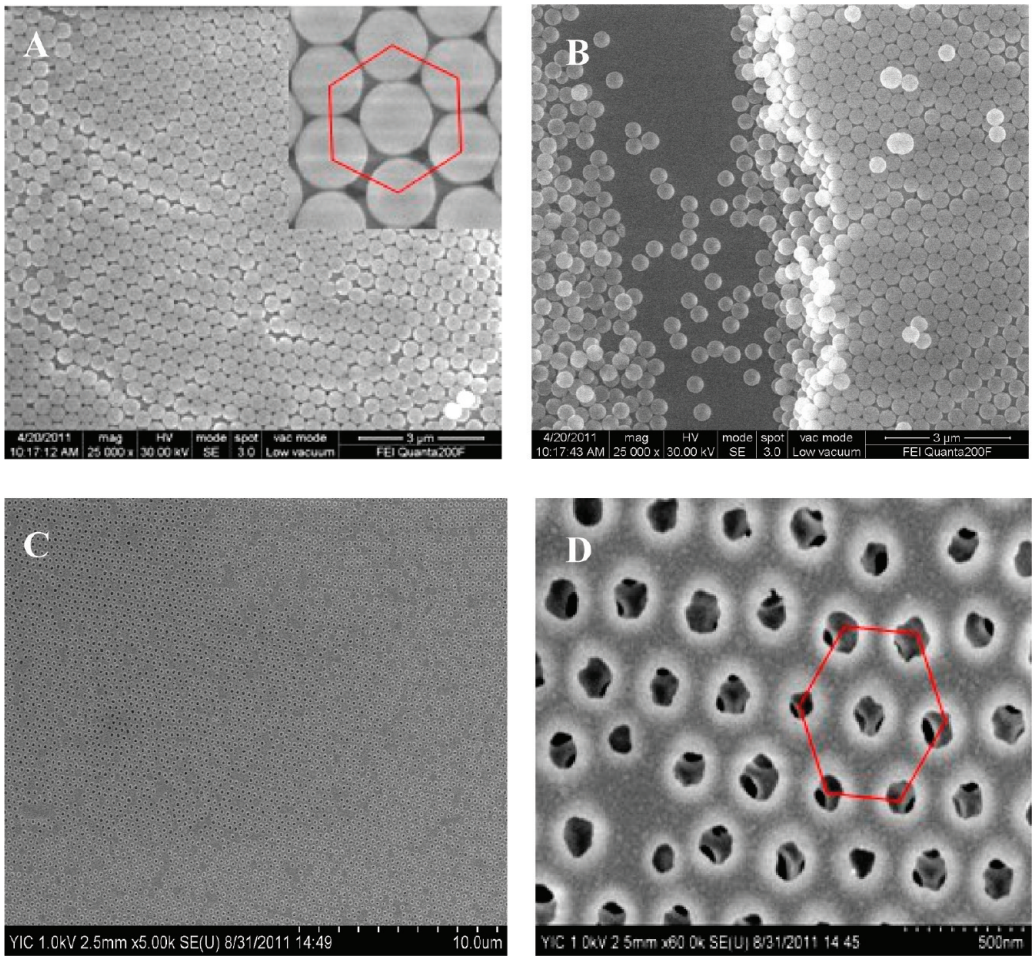


**Figure 2.** SEM images of photonic colloidal crystal molding (A) and its cross-section (B) and the MIPH (C, D).

and TEOS (9.4 mL) and $NH_3 \cdot H_2O$ (15 mL) were slowly added with intense stirring at room temperature for 12 h. Silica particles were obtained by centrifugation and rinsing using anhydrous ethanol four times to wash off residues. Then, the obtained silica particles were fully dispersed in anhydrous ethanol by an ultrasonic bath with a weight concentration of approximately 3% for use.

**Preparation of Silica Photonic Crystal Moldings.** The treated glass slides were put vertically into each test tube, and then the obtained monodisperse silica particles were added into the test tubes. To obtain ideal silica colloidal crystal moldings, these test tubes were placed in a quiet environment. The silica colloidal crystal moldings were formed on both sides of each glass slide after complete volatilization of ethanol.

**Fabrication of MIPH.** The template molecule of vanillin (2 mmol), the functional monomer of MAA (8 mmol), and the cross-linker of EGDMA (2.4 mmol) were dissolved in methanol (1.5 mL) and then were stored overnight in a refrigerator (4 °C) for sufficient complexation. The initiator of AIBN (0.122 mmol) was added for the preparation of precursor solution and then sonicated and degassed with nitrogen for 10 min to remove the dissolved oxygen. The silica colloidal crystal moldings and PMMA substrates were held tightly together forming the "sandwich structure" and then dipped into the prepared precursor solution. The precursor solution would be infiltrated into the space of the sandwich structure by capillary forces. The sandwich structure was taken out until the colloidal crystal became transparent. The interspace of the used colloidal crystal moldings was fully filled with the precursor solution. Photopolymerization was performed in an ice bath under UV light at 365 nm for 2 h. Then, the sandwich structures were immersed into 3% hydrofluoric acid solution for 8−10 h to separate double slides and etch the silica particles. Meanwhile, fortunately, the substrate of PMMA exhibited resistance without damage in the hydrofluoric acid solution; in contrast, common glass and quartz glass would be etched. After it was eluted in methanol for 2 h to remove the template molecule of vanillin, the MIPH was formed on the PMMA slides and then purged with a phosphate buffer solution (PBS, pH 7.6, 0.01 mol $L^{-1}$) for 6 h for use. As a control, the nonimprinted photonic hydrogel (NIPH) was also prepared using the same procedure but in the absence of vanillin template molecules.

**Scanning Electron Microscopy (SEM) of MIPH.** The morphological features of silica colloidal crystal moldings and MIPH were examined by SEM (Quanta 200F, FEI, Hillsboro, OR). The samples were sprinkled onto double-sided tape and sputter-coated with a 5 nm thick gold layer.

**Optical Properties of MIPH.** The optical properties of silica photonic crystal moldings and MIPH were recorded by a digital camera, and the sensing of MIPH was determined by a UV−vis spectrometer (TU-1901, Beijing, China).

**Selectivity and Recognition Specificity Studies of MIPH.** The solutions of the analytes (vanillin, methyl vanillin, or ethyl vanillin) were prepared at concentrations of $10^{-12}$, $10^{-9}$, $10^{-6}$, and $10^{-3}$ mol $L^{-1}$ in buffer solution, respectively. The MIPH was dipped into the prepared analyte buffer solutions one after another from low to high concentrations, and the Bragg diffraction wavelength shift was measured using the UV−vis spectrometer.

**Adsorption Analysis of MIPH.** The films (10 mg) were obtained from the MIPH and added into the vanillin buffer solution (0.01, 0.02, 0.04, 0.06, 0.08, and 0.10 mmol $L^{-1}$). The mixtures were shaken at 30 °C for 12 h and then were centrifuged for 10 min and filtered. The free vanillin concentration on the supernatant was analyzed by UV−vis at the wavelength of 229 nm. The amount of vanillin bound to the MIPH was calculated by subtracting the free amount from its initially added

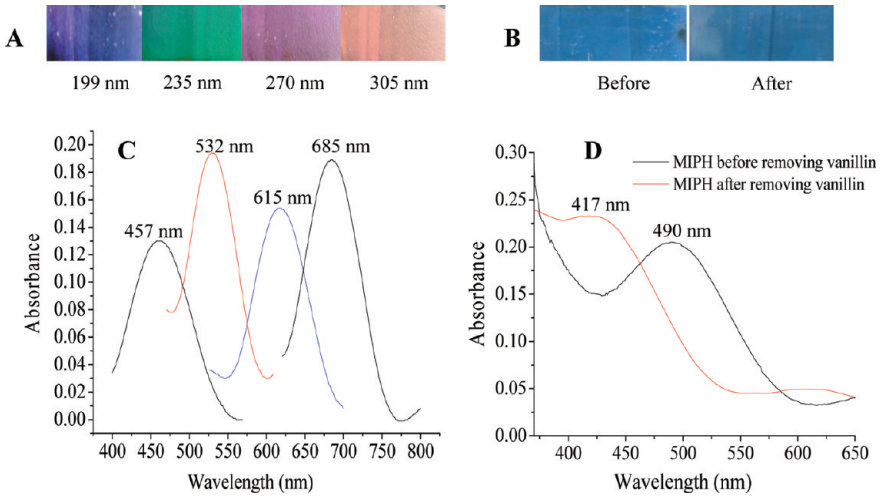


**Figure 3.** Colors and UV absorption of the photonic crystal moldings (A, C) and the MIPH (B, D). The MIPH was fabricated from the photonic crystal molding of 190 nm.

amount of vanillin. To gain insight inyo the adsorption mechanism of vanillin onto the MIPH, Langmuir, Freundlich, and Scatchard models were used to fit the adsorption processes.

## RESULTS AND DISCUSSION

**Fabrication of Vanillin MIPH.** The vanillin MIPH was prepared by a noncovalent, self-assembly approach. Figure 1 illustrates the steps of preparation: synthesis of silica particles, preparation of silica colloidal crystals molding, preparation of sandwich structure, formation of the inverse opals, and construction of vanillin MIPH. The silica particles were synthesized according to the classic Stöber method,[28] and the silica photonic crystals were prepared by vertical deposition on glass substrates and were used as moldings for the formation of 3D highly ordered, interconnected macroporous structures. It should be noted that the irregular deposition layer would appear on the silica colloidal crystal moldings, which may result from the temperature difference or noise during the formation process of photonic crystal moldings. Thus, constant temperature and a quiet environment are necessary. For obtaining MIPH, the silica particles and template molecules of vanillin should be removed. The spaces formed by the removal of silica particles and the embedded vanillin molecules from the imprinted polymer matrix were 3D highly ordered and interconnected macroporous. The MIPH with specific nanocavities could specifically and easily interact with the vanillin molecule through noncovalent interactions.

**Morphology of Silica Photonic Crystal Molding and MIPH.** Figure 2 displays typical SEM images of the colloidal crystal molding and MIPH. As can be seen in Figure 2A, the silica colloidal particle was arranged in a close-packed way, evidenced by a random sphere touching another six in one layer. The photonic crystal molding was also found to be highly 3D ordered with a hexagonal symmetry (Figure 2A). Although such morphology confirms a relatively regular close-packed array, it cannot be used to distinguish the difference between the face-centered cubic (fcc) (ABCABC...) and hexagonal close-packed (ABABAB...) structures.[29] However, theoretical calculations have indicated that the fcc structure and particular (111) lattice is energetically preferable for experiments.[29] It is obvious that the photonic crystals are arranged over the entire surface with (111), parallel to the substrate. Figure 2B presents a cross-section image of the photonic crystal molding, clearly showing that the film has about nine layers assembled layer by layer. After removal of the opal molding and silica particles, the structures of the opal structure of photonic crystal molding were duplicated, and the 3D highly ordered and interconnected macroporous structure was well maintained with the (111) orientation planes (Figure 2C,D). That is, MIPH, the inverse opal hydrogel on the PMMA, was successfully fabricated.

**Optical Properties of MIPH.** The 3D photonic crystal is an artificial periodic dielectric structure possessing photonic band gaps, namely, frequency stop bands, in which the density of photonic states tends to zero.[30] It obeys Bragg's law when there is a visible light incidence on the structure. For the Bragg diffraction peak, the maximum wavelength ($\lambda_{max}$) is determined by the Bragg diffraction law as

$$\lambda_{max} = 2d_{hkl}(n_{eff} - \sin^2\theta)^{1/2} \quad (1)$$

where $d_{hkl}$ is the interplanar distance of two neighboring layers along the incident direction, $n_{eff}$ is the effective refractive index, and $\theta$ is the incidence angle of light. Because of the fcc structure, $d_{111} = 0.816D$ ($D$ is the diameter of silica particles). The effective refractive index ($n_{eff}$) can be expressed as

$$n_{eff} = [n_{sp}^2 f + n_{vo}^2(1 - f)]^{1/2} \quad (2)$$

where $n_{sp} = 1.45$ and $n_{vo} = 1.0$ are the refractive index of silica particles and air, respectively. $f = 0.746$ is the filling ratio of silica particles. Because of vertical incidence, the incidence angle of light ($\theta$) is 90°. Therefore, eq 1 can then be expressed as eq 3:

$$\lambda_{max} = 20 \times 0.816 \times D \times [n_{sp}^2 f + n_{vo}^2(1 - f)\sin^2\theta]^{1/2} \quad (3)$$

On the basis of eq 2, eq 3 can further be changed into eq 4:

$$\lambda_{max} = 2.20D \quad (4)$$

Equation 4 shows that the wavelength ($\lambda_{max}$) could be varied by changing the diameter of the silica particles. In this study, the diameters of silica particles were 199, 235, 270, and 305 nm for different photonic crystal moldings (Figure 3A), and the calculated wavelengths ($\lambda_{max}$) were 438, 517, 594, and 671 nm, respectively. Accordingly, the adopted experimental wave-


dx.doi.org/10.1021/jf204736p | J. Agric. Food Chem. 2012, 60, 1921−1928

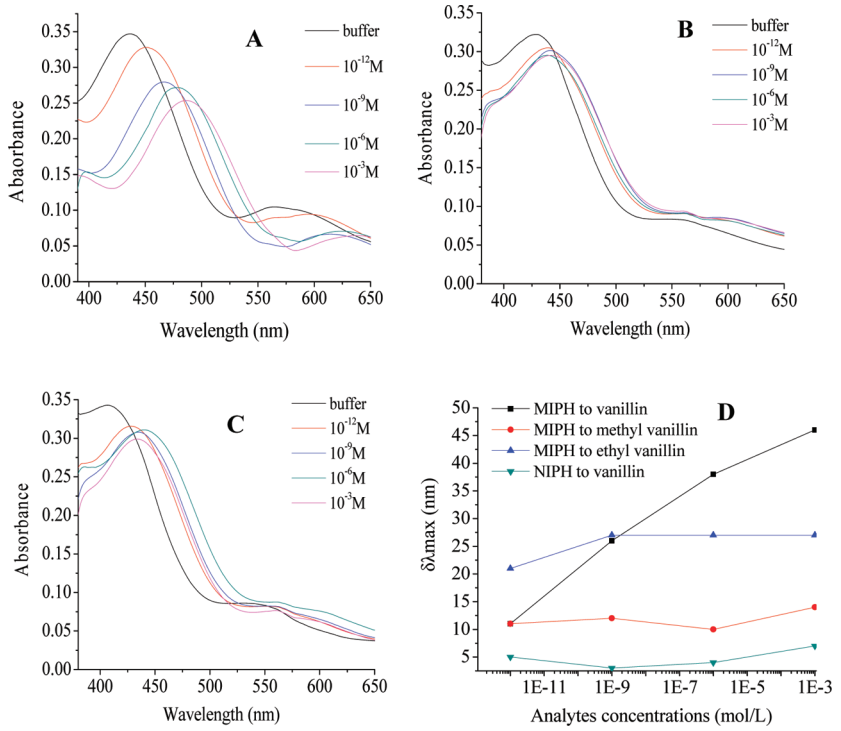


**Figure 4.** Optical response of the MIPH to different concentrations of vanillin (A), methyl vanillin (B), and ethyl vanillin (C) solution and plots of Bragg diffraction shifts of the MIPH to concentrations (D).

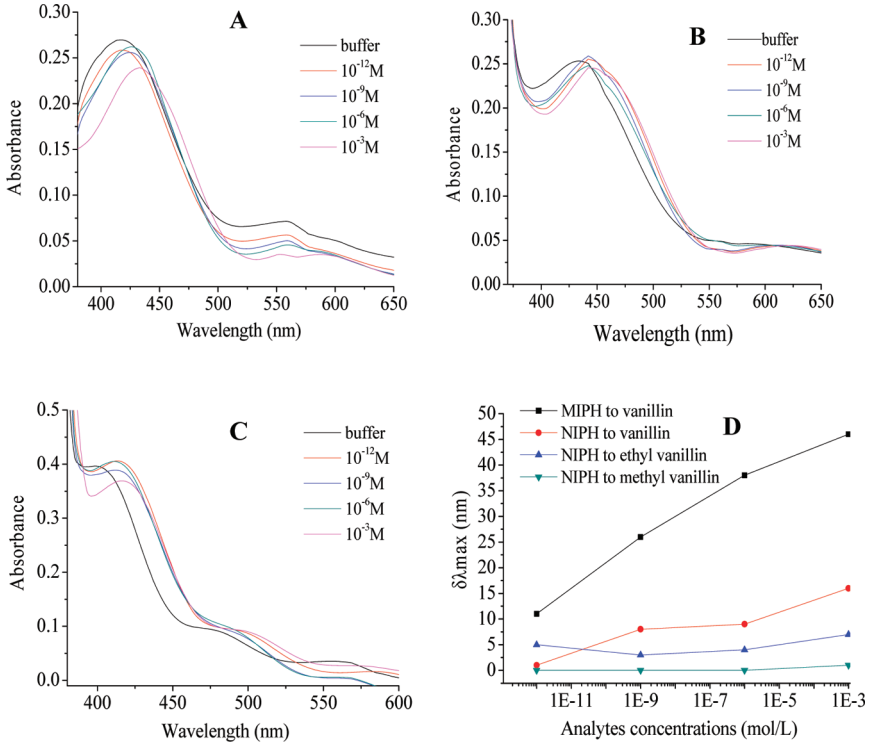


**Figure 5.** Optical response of the NIPH to different concentrations of vanillin (A), methyl vanillin (B), and ethyl vanillin (C) solution and plots of Bragg diffraction shifts of the NIPH to concentrations (D).

lengths ($\lambda_{max}$) were 457, 532, 615, and 685 nm, respectively (Figure 3C). The results indicated that the wavelength ($\lambda_{max}$) of photonic crystal moldings was red-shifted with an increase in the diameter of silica particles. By plotting the wavelength ($\lambda_{max}$) against the diameter of the silica particles, a linear plot ($y$ = 2.165$x$ + 35.65) was yielded with a higher correlation coefficient ($R^2$ = 0.9990). There is only a little difference between the experimental slope (2.165) and the Bragg slope (2.20), and the standard error of $\lambda_{max}$ between the experimental and the calculation values was within 5%. All of this indicated that the diffraction of the photonic crystal molding obeyed the Bragg diffraction law. Because of the Bragg diffraction property


dx.doi.org/10.1021/jf204736p | J. Agric. Food Chem. 2012, 60, 1921−1928

and 3D ordered structure, the different structural colors of photonic crystal moldings were observed in the range from blue to light red (Figure 3A).

The MIPH was fabricated from the photonic crystal molding of 199 nm. The results of structural colors are shown in Figure 3B. It can be seen that the color of MIPH film was different from the photonic crystal molding, which may be because of the different size between the silica particles and nanocavities of MIPH film. Because of 3D network structures, the MIPH could be swelled or shrunken under environmental stimuli, and the Bragg diffraction (a readable optical signal) of the MIPH was shifted from 417 to 490 nm after rebinding of vanillin (Figure 3D).

**Molecular Selectivity and Sensing Specificity of the MIPH.** The molecular selectivity and sensing specificity of the MIPH were investigated by using vanillin as the template molecule, as well as methyl vanillin and ethyl vanillin as the control compounds. Figure 4 show the results of the Bragg diffraction shift and optical response of the MIPH to these compounds. As shown in Figure 4A, the Bragg diffraction peak of the MIPH shifted regularly to the longer wavelength region with increasing concentrations of vanillin. The wavelength increased from 451 to 486 nm with the concentration increase of vanillin from $10^{-12}$ to $10^{-3}$ mol $L^{-1}$ within 60 s. However, there was almost no Bragg diffractive peak shift in methyl vanillin and ethyl vanillin buffer solutions, as seen in Figure 4B,C. The Bragg diffractive shifts against vanillin concentration are shown in Figure 4D. It can also be observed that the Bragg diffractive shifts of the MIPH gradually increased with the increasing concentration of vanillin. In contrast, the Bragg diffractive shifts fluctuated irregularly or remained nearly constant for the methyl vanillin and ethyl vanillin solutions. These results suggested that the MIPH possessed highly specific and sensitive recognition ability for the template molecule of vanillin.

The high specificity of MIPH mainly depends on two factors, the molecular dimension and shape of the template and the matching degree of the bonding sites. The reason is believed to be that the selectivity of the MIPH film for vanillin was clearly induced during the molecular imprinting process. Because of the complementary shape, size, and interaction sites with the formed binding cavities, only vanillin rather than other molecules can specifically occupy the imprinted nanocavities within the MIPH film and cause the volume change of the hydrogel film, thereby inducing the shift of the Bragg diffraction peak. Thus, the MIPH was indicated to be highly specific to vanillin.

To gain further insight into the selectivity and recognition specificity of MIPH, the NIPH was also soaked in buffer solutions containing vanillin, methyl vanillin, and ethyl vanillin, respectively. As shown in Figure 5, the results indicated that the Bragg diffractive shifts of the NIPH were greatly different from those of the MIPH with irregular fluctuation or near constancy for vanillin, methyl vanillin, and ethyl vanillin. It is very likely that there are no specific binding sites in the NIPH.

The results described above clearly indicated that the microenvironments created by molecular imprinting are responsible for the observations of vanillin MIPH. The MIPH not only offered remarkable sensing characteristics surpassing NIPH but also delicately discriminated between the very similar structures to vanillin. Thus, it can be concluded that the overall effect of shape, size, and interaction sites is vital for the highly selective molecular recognition process of MIPH.

**Adsorption Analysis of MIPH.** The binding capacities of vanillin onto MIPH were analyzed, and the results are shown in Figure 6A. It was observed that the adsorption amount of

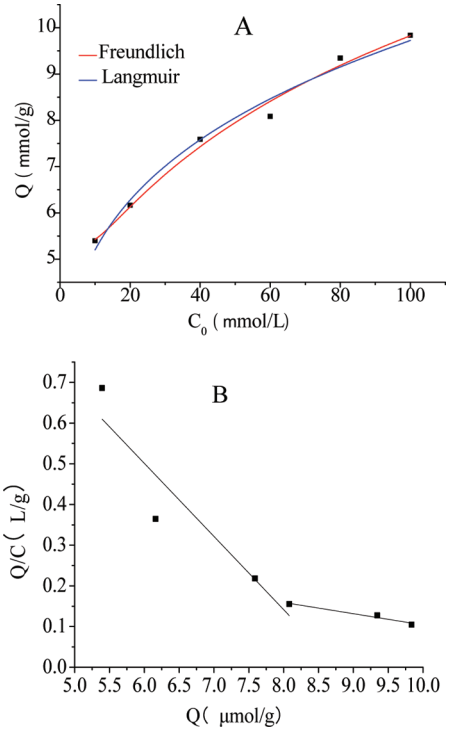


**Figure 6.** (A) Adsorption isotherm data and comparison of Langmuir and Freundlich isotherm models for vanillin adsorption onto MIPH. (B) Scatchard plots of the MIPH.

vanillin onto MIPH increased with an increasing initial vanillin concentration. This result suggested that the MIPH possessed a large number of specific binding sites within the highly ordered 3D macroporous structure. The specific binding sites play a predominant role for the adsorption capacity and favor the transfer of vanillin from the liquid to the MIPH. The adsorption capacity was increased quickly and approached equilibrium at the lower and higher concentrations, respectively. When these binding sites and nanocavities in the structure were occupied, it became difficult for vanillin to implant into the interior of MIPH. This would cause the adsorption to slow at higher concentrations. Also, it was found that the adsorption capacity of the NIPH was very low (data not shown), probably due to no specific binding sites in the NIPH for vanillin.

To gain insight into the adsorption mechanism of MIPH, the adsorption data were analyzed by Langmuir, Freundlich, and Scathard isotherm models.[31,32]

$$\text{Langmuir isotherm model:}\quad C_e/Q_e = C_e/Q_m + 1/Q_m K_L \tag{5}$$

$$\text{Freundlich isotherm model:}\quad \ln Q_e = (1/n)\ln C_e + \ln K_f \tag{6}$$

$$\text{Scathard isotherm model:}\quad Q_e/C_e = (Q_m - Q_e)/K_s \tag{7}$$


dx.doi.org/10.1021/jf204736p | J. Agric. Food Chem. 2012, 60, 1921−1928

$C_e$ is the equilibrium concentration of vanillin, $Q_e$ is the adsorption capacity of MIPH, $Q_m$ and $K_f$ are the maximum adsorption capacity of MIPH, $1/n$ is the adsorption intensity, and $K_L$ and $K_S$ are the Langmuir and Scathard model constants, respectively. The results of Langmuir and Freundlich isotherms are shown in Figure 6A and Table 1. It can be observed that the

**Table 1. Isotherm Model Constants for the MIPH**

| isotherm model | constant | MIPH |
|---|---|---|
| Langmuir | $R^2$ | 0.988 |
| | $Q_m$ | 10.86 |
| | $K$ | 0.08 |
| Freundlich | $R^2$ | 0.983 |
| | $K_f$ | 2.78 |
| | $1/n$ | 0.27 |

Langmuir isotherm model yielded a better fit than that by the Freundlich model with correlation coefficients ($R^2$) of 0.988. Thus, the Langmuir isotherm model is suitable to the adsorption. According to the Scatchard equation, there were two distinct sections within the plot, which could be regarded as straight lines (Figure 6B). The results indicated that there were two types of binding sites for MIPH, and the rebinding sites were mainly dependent on hydrogen bonding. From the slope and intercept of the plot, the $Q_{m1}$ and $K_{s1}$ were 8.827 $\mu$mol $g^{-1}$ and 5.586 $\mu$mol $L^{-1}$, respectively, and the $Q_{m2}$ and $K_{s2}$ were 14.074 $\mu$mol $g^{-1}$ and 37.04 $\mu$mol $L^{-1}$, respectively. The results indicated that the MIPH had higher adsorption capacity, which also verified its sensing specificity for vanillin.

**Response Characteristic, Reproducibility, and Storage Stability of MIPH.** The response characteristic was investigated by immersing MIPH into vanillin solution ($10^{-3}$ mol $L^{-1}$) for 15, 30, 45, 60, and 75 s, respectively. The wavelength change is shown in Figure 7A. The results indicated that the MIPH exhibited rapid response to vanillin and reached adsorptive equilibrium within 60 s. This might be attributed to two reasons. The first one is that the homogeneous layers and the interconnected macroporous structure make vanillin diffuse into the MIPH and occupy the binding sites easily. The second one is that the high surface-to-volume ratio and special recognition sites are another driving force to promote diffusion of vanillin from bulk solutions into the MIPH. The recoverability of MIPH was studied by an elution and rebinding method. That is, the MIPH was eluted using methanol and immersed into vanillin buffer solution ($10^{-3}$ mol $L^{-1}$) for rebinding. As seen from Figure 7B, the results within five cycles suggested that the MIPH possessed an ideal recoverability. Furthermore, the MIPH film was indicated as being excellently reproducible due to the recoverability of five cycles with the standard error within 5%. As for the long time stability, the MIPH film still gave almost consistent detection observations when it was stored at 4 °C in a refrigerator for 3 months.

In summary, a novel label-free colorimetric sensing method for the convenient and highly sensitive detection of vanillin based on the combination of molecular imprinting and photonic hydrogel was successfully developed. Because of the simultaneous possession of high sensitivity and specificity, quick response, good regenerating ability, direct transduction, and label-free measurement, the MIPH sensory platform is hopefully developed for the routine monitoring of on-site food quality control and market surveillance. Furthermore, to develop and perfect the smart sensor that can directly transfer the molecular recognition process into a readable signal and realize practical applications, other techniques such as transduction, computer, and biological elements would be integrated into the sensor. We believe that such sensors would be suitable not only for laboratory assays but also for in-field fast and real-time detection of trace analytes in the future.

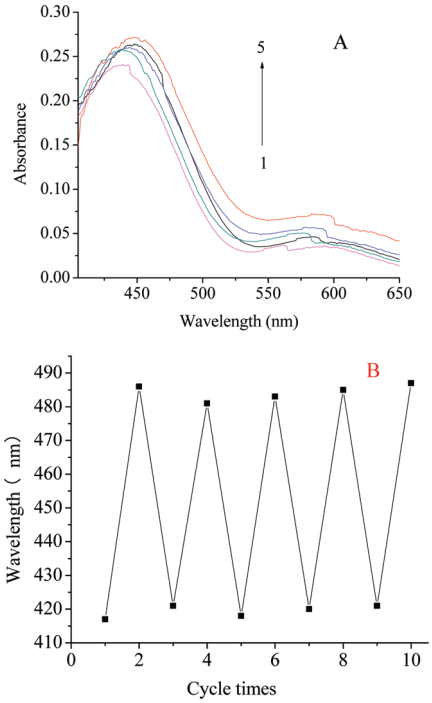


**Figure 7.** (A) Response (times for lines 1−5: 15, 30, 45, 60, and 75 s) of MIPH in vanillin solution ($10^{-3}$ mol $L^{-1}$). (B) Recoverability of the MIPH dipped in a PBS containing vanillin and recovered in a PBS with vanillin after elution.

## AUTHOR INFORMATION


### Corresponding Author

*Phone/fax: +86 791 6634810. E-mail: huaxiong100@yahoo.com.cn.

### Author Contributions

‖Equally contributed to this work.



### Funding

This work was supported by the National Natural Science Foundation of China (31160317, 21105117, and 20975089), the Programs of State Key Laboratory of Food Science and Technology of Nanchang University (SKLF-KF-201006), and the Innovation Projects of the Chinese Academy of Sciences (KZCX2-EW-206).


### Notes

The authors declare no competing financial interest.

## REFERENCES


(1) Ni, Y. N.; Zhang, G. W.; Kokot, S. Simultaneous spectrophotometric determination of maltol, ethyl maltol, vanillin and ethyl vanillin in foods by multivariate calibration and artificial neural networks. *Food Chem.* **2005**, *89*, 465−473.

(2) AOAC. *Official Methods of Analysis of AOAC*; AOAC: Arlington, VA, 1990.

(3) DeJagerd, L. S.; Perfetti, G. A.; Diachenko, G. W. Comparison of headspace-SPME-GC-MS and LC-MS for the detection and

quantification of coumarin, vanillin, and ethyl vanillin in vanilla extract products. *Food Chem.* **2008**, *107*, 1701−1709.
(4) Waliszewski, K. N.; Pardio, V. T.; Ovando, S. L. A simple and rapid HPLC technique for vanillin determination in alcohol extract. *Food Chem.* **2007**, *101*, 1059−1062.
(5) Ohashi, M.; Omae, H.; Hashida, M.; Sowa, Y.; Imai, S. Determination of vanillin and related flavor compounds in cococa drink by capillary electrophoresis. *J. Chromatogr., A* **2007**, *1138*, 262−267.
(6) Chen, L. X.; Xu, S. F.; Li, J. H. Recent advances in molecular imprinting technology: current status, challenges and highlighted applications. *Chem. Soc. Rev.* **2011**, *40*, 2922−2942.
(7) Tamayo, F. G.; Turiel, E.; Martin-Esteban, A. Molecularly imprinted polymers for solid-phase extraction and solid-phase microextraction: Recent developments and future trends. *J. Chromatogr., A* **2007**, *1152*, 32−40.
(8) Mahony, J. O.; Nolan, K.; Smyth, M. R.; Mizaikoff, B. Molecularly imprinted polymers potential and challenges in analytical chemistry. *Anal. Chim. Acta* **2005**, *534*, 31−39.
(9) Xu, S. F.; Chen, L. X.; Li, J. H. Molecularly imprinted core-shell nanoparticles for determination of trace atrazine by reversible addition-fragmentation chain transfer surface imprinting. *J. Mater. Chem.* **2011**, *21*, 4363−4351.
(10) Kitahara, K. I.; Yoshihama, I.; Hanada, T.; Kobuba, H.; Arai, S. Synthesis of monodispersed molecularly imprinted polymer particles for high-performance liquid chromatographic separation of cholesterol using templating polymerization in porous silica gel bound with cholesterol molecules on its surface. *J. Chromatogr., A* **2010**, *1217*, 7249−7254.
(11) Moreira, F. T. C.; Kamel, A. H.; Guerreiro, J. R. L.; Sales, M. G. F. Man-tailored biomimetic sensor of molecularly imprinted materials for the potentiometric measurement of oxytetracycline. *Biosens. Bioelectron.* **2010**, *26*, 566−574.
(12) Moreira, F. T. C.; Sales, M. G. F. Biomimetic sensors of molecularly-imprinted polymers for chlorpromazine determination. *Mater. Sci. Eng., C* **2011**, *31*, 1121−1128.
(13) Belmont, A. S.; Jaeger, S.; Knopp, D.; Niessner, R.; Gauglitz, G.; Haupt, K. Molecularly imprinted polymers films for reflectometric interference spectroscopic sensors. *Biosens. Bioelectron.* **2007**, *22*, 3267−3272.
(14) Schwarz, L. J.; Danylec, B.; Yang, Y. Z.; Harris, S. J.; Boysen, R. I.; Hearn, M. T. W. Enrichment of (*E*)-resveratrol from peanut byproduct with molecularly imprinted polymers. *J. Agric. Food Chem.* **2011**, *59*, 3539−3543.
(15) Ramström, O.; Skudar, K.; Haines, J.; Patel, P.; Brüggemann, O. Food analyses using molecularly imprinted polymers. *J. Agric. Food Chem.* **2001**, *49*, 2105−2114.
(16) Curcio, M.; Puoci, F.; Cirillo, G.; Iemma, F.; Spizzirri, U. G.; Picci, N. Selective determination of melamine in aqueous medium by molecularly imprinted solid phase extraction. *J. Agric. Food Chem.* **2010**, *58*, 11883−11887.
(17) Alizadeh, T.; Ganjali, M. R.; Zare, M.; Norouzi, P. Selective determination of chloramphenicol at trace level in milk samples by the electrode modified with molecularly imprinted polymer. *Food Chem.* **2012**, *130*, 1108−1114.
(18) Nair, R. V.; Vijaya, R. Photonic crystal sensors: an overview. *Prog. Quantum Electron.* **2010**, *34*, 89−134.
(19) Kim, S. H.; Park, H. S.; Choi, J. H.; Shim, J. W.; Yang, S. M. Integration of colloidal photonic crystals toward miniaturized spectrometers. *Adv. Mater.* **2010**, *22*, 946−950.
(20) Comoretto, D.; Grassi, R.; Marabelli, F.; Andreani, L. C. Growth and optical studies of opal films as three-dimensional photonic crystal. *Mater. Sci. Eng., C* **2003**, *23*, 61−65.
(21) Wu, Z.; Hu, X. B.; Tao, C. A.; Li, Y.; Liu, J.; Yang, C. D.; Shen, D. Z.; Li, G. T. Direct and label-free detection of cholic acid based on molecularly imprinted photonic hydrogels. *J. Mater. Chem.* **2008**, *18*, 5452−5458.
(22) Hu, X. B.; Li, G. T.; Li, M. H.; Huang, J.; Li, Y.; Gao, Y. B.; Zhang, Y. H. Ultrasensitive specific stimulant assay based on molecularly imprinted photonic hydrogels. *Adv. Funct. Mater.* **2008**, *18*, 575−583.
(23) Hu, X. B.; Li, G. T.; Huang, J.; Zhang, D.; Qiu, Y. Construction of self-reporting specific chemical sensors with high sensitivity. *Adv. Mater.* **2007**, *19*, 4327−4332.
(24) Braun, P. V.; Shin, J.; Lee, W. Fast response photonic crystal pH sensor based on template photo-polymerized hydrogel inverse opal. *Sens. Actuators, B* **2010**, *150*, 183−190.
(25) Asher, S. A.; Sharma, A. C.; Goponenko, A. V.; Ward, M. M. Photonic crystal aqueous metal cation sensing materials. *Anal. Chem.* **2003**, *75*, 1676−1683.
(26) Holtz, J. H.; Asher, S. A. Intelligent polymerized crystalline colloidal array hydrogel film chemical sensing materials. *Nature* **1997**, *389*, 829−832.
(27) Barry, R. A.; Wiltzius, P. Humidity-sensing inverse opal hydrogels. *Langmuir* **2006**, *22*, 1369−1374.
(28) Stöber, W.; Fink, A.; Bohn, E. Controlled growth of monodisperse silica spheres in the micron size range. *J. Colloid Interface Sci.* **1968**, *26*, 62−69.
(29) Sinitskii, A. S.; Knot'ko, A. V.; Tretyakov, Y. D. Silica photonic crysal: synthesis and optical properties. *Solid State Ionics* **2004**, *172*, 477−479.
(30) Johnson, N. P.; McComb, D. W.; Richel, A.; Treble, B. M.; Rue, R. M. D. L. Synthesis and optical properties of opal and inverse opal photonic crystal. *Synth. Met.* **2001**, *116*, 469−473.
(31) Chen, C. Y.; Wang, C. H.; Chen, A. H. Recognition of molecularly imprinted polymers for a quaternary alkaloid of berberine. *Talanta* **2011**, *84*, 1038−1046.
(32) Zhu, G. F.; Fan, J.; Gao, Y. B.; Gao, X.; Wang, J. J. Synthesis of surface molecularly imprinted polymer and the selective solid phase extraction of imidazole from its structural analogs. *Talanta* **2011**, *84*, 1124−1132.